Effect of atomic order on the martensitic and magnetic transformations in Ni–Mn–Ga ferromagnetic shape memory alloys

2010 J. Phys.: Condens. Matter 22 166001

(http://iopscience.iop.org/0953-8984/22/16/166001)

J. Phys.: Condens. Matter **22** (2010) 166001 (7pp) doi:10.1088/0953-8984/22/16/166001

Effect of atomic order on the martensitic and magnetic transformations in Ni–Mn–Ga ferromagnetic shape memory alloys

V Sánchez-Alarcos[1], J I Pérez-Landazábal[1], V Recarte[1], J A Rodríguez-Velamazán[2,3] and V A Chernenko[4]

[1] Departamento de Física, Universidad Pública de Navarra, Campus de Arrosadía, E-31006 Pamplona, Spain
[2] Instituto de Ciencia de Materiales de Aragón, CSIC—Universidad de Zaragoza, E-50009 Zaragoza, Spain
[3] Institut Laue-Langevin, CRG's D1B D15, F-38042 Grenoble, France
[4] Departamento de Electricidad y Electrónica, Universidad del País Vasco, PO Box 644, E-48080 Bilbao, Spain

E-mail: vicente.sanchez@unavarra.es

Received 11 February 2010, in final form 15 March 2010
Published 6 April 2010
Online at stacks.iop.org/JPhysCM/22/166001

Abstract
The influence of long-range $L2_1$ atomic order on the martensitic and magnetic transformations of Ni–Mn–Ga shape memory alloys has been investigated. In order to correlate the structural and magnetic transformation temperatures with the atomic order, calorimetric, magnetic and neutron diffraction measurements have been performed on polycrystalline and single-crystalline alloys subjected to different thermal treatments. It is found that both transformation temperatures increase with increasing atomic order, showing exactly the same linear dependence on the degree of $L2_1$ atomic order. A quantitative correlation between atomic order and transformation temperatures has been established, from which the effect of atomic order on the relative stability between the structural phases has been quantified. On the other hand, the kinetics of the post-quench ordering process taking place in these alloys has been studied. It is shown that the activation energy of the ordering process agrees quite well with the activation energy of the Mn self-diffusion process.

1. Introduction

Ferromagnetic shape memory alloys (FSMA) have received an enormous amount of attention over the last few years since, together with the properties of the conventional shape memory alloy, such as superelasticity and shape memory behavior, some other peculiar properties have been found to arise from the coupling between structure and magnetism. The most interesting feature is the fact that the thermoelastic martensitic transformation (MT) taking place in these alloys gives rise to a crystallographic domain structure linked to the magnetic domain structure in such a way that the application of a magnetic field may promote extremely large magnetic-field-induced strains (MFIS) [1, 2]. Alongside the MFIS effect, several other interesting properties are being investigated in FSMA because of their potential applications, namely the magnetocaloric effect (MCE) and magnetoresistance (MR) [3, 4].

Up to now, the highest MFIS, as large as 10%, have been obtained in near-stoichiometric Ni_2MnGa Heusler alloys, by far the most studied FSMA [5]. In such alloys, the MT is driven by a Jahn–Teller mechanism [6] and takes place from a high temperature phase showing a Heusler $L2_1$ crystal structure (austenite) to a lower symmetry low temperature phase (martensite) showing several crystallographic structures depending on composition [7, 8]. The MT temperature (T_m)

strongly depends on composition [9] and the compositional dependence has been traditionally described as a function of the electron to atom ratio, e/a, just as it occurs in the Hume-Rothery compounds [10]. It is also well known that the ferromagnetism in these alloys is due to the ferromagnetic coupling between the Mn atoms, in which the magnetic moment of the alloy is mainly located, and, to a lesser extent, due to the Ni–Mn coupling [11, 12].

The change of long-range atomic order affects both the MT and the magnetic properties due to the modification of both the electronic structure and the lattice site occupancy by the magnetic atoms. It has been established that Ni–Mn–Ga alloys solidify from the melt to a cubic B2 structure (nearest-neighbors atomic order) and that the austenitic $L2_1$ structure (next-nearest-neighbors atomic order) is reached through a B2–$L2_1$ ordering process taking place on further cooling. On cooling below T_m, the austenite atomic order is inherited by the martensite due to the diffusionless character of the MT [13–17]. The effect of the atomic order on the MT temperature in near-stoichiometric Ni–Mn–Ga alloys has been studied in several works, in which the atomic order was changed either by applying thermal treatments or by modifying the alloy composition [17–22]. High temperature annealing followed by quenching is one of the most common thermal treatments used to modify the atomic order. It has been shown that T_m increases with the increasing degree of $L2_1$ atomic order, which, in turn, increases as the result of both the quenching temperature decrease and as a consequence of moderate-temperature post-quench treatments. The Curie temperature (T_C) and the high and low field magnetization have also been shown to increase with the increasing next-nearest-neighbor order under such thermal treatments [17, 22]. Similar magnetic results were obtained from experimental and theoretical studies on the modification of atomic order by means of composition variation [21, 23]. This behavior is explained as a consequence of the variation of the magnetic moment of the alloys depending on the position of the Mn atoms, which couple antiferromagnetically when they are nearest-neighbors (Mn atoms on the Ga positions) and ferromagnetically when they are next-nearest-neighbors (Mn atoms in the Mn sublattice).

Despite the influence of atomic order on both the structural and magnetic transformations in Ni–Mn–Ga alloys being quite well understood, there is still a lack of quantitative results. In this respect, a quantitative study of the effect of atomic order on both T_m and T_C has been carried out in this work. In particular, a numerical correlation between transformation temperatures and atomic order has been established from magnetic, calorimetric and neutron diffraction measurements performed on both polycrystalline and single-crystalline alloys subjected to different thermal treatments. On the basis of the experimental results, the influence of magnetism on the MT and the nature of the post-quench ordering process are also discussed.

2. Experimental details

The study has been carried out on two alloys of similar composition, an $Ni_{49.5}Mn_{28.5}Ga_{22}$ (at.%) polycrystalline alloy and an $Ni_{49.4}Mn_{27.7}Ga_{22.9}$ (at.%) single-crystalline alloy (hereafter referred to PC and SC alloys, respectively). The PC alloy was prepared from high-purity elements by arc melting under a protective Ar atmosphere and homogenized in a vacuum quartz ampoule at 1273 K for 24 h. The SC alloy was prepared by the Bridgman technique. In order to modify the long-range atomic order, the PC alloy was subjected to annealing treatments in a vertical furnace for 30 min at 873, 973, 1073 and 1173 K followed by quenching into ice water. The SC alloy was annealed at 1173 K, quenched into ice water and then subjected to two consecutive post-quenching heating treatments up to 600 and 673 K at a heating rate of 10 K min^{-1}. Differential scanning calorimetry (DSC) measurements at a heating/cooling rate of 10 K min^{-1} were carried out with a TA Q100 DSC to obtain the transformation temperatures. A Quantum Design MPMS XL-7 superconducting quantum interference device (SQUID) magnetometer [24] was used to measure the saturation magnetization. The degree of atomic order was estimated from neutron diffraction experiments carried out at the ILL (Institute Laue-Langevin). Powder neutron diffraction measurements were conducted on the PC alloy quenched from 873, 1073 and 1173 K on the D1B diffractometer at a wavelength of 1.28 Å. In the case of the SC alloy, the neutron diffraction measurements were performed on the single-crystal D15 diffractometer. The instrument, provided with a closed-cycle cryostat, was used in the four-circle configuration at a wavelength of 1.173 Å.

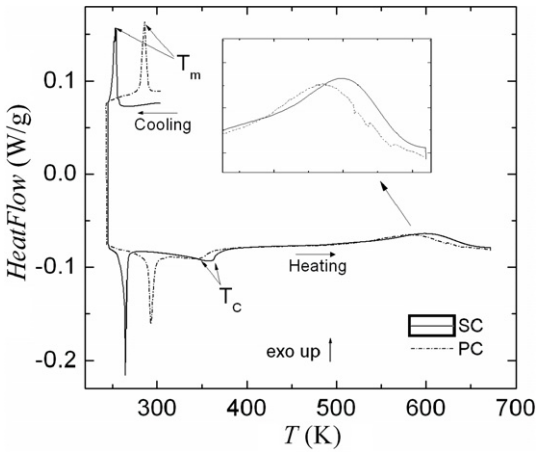

Figure 1. DSC thermograms obtained on both PC and SC samples quenched from 1173 K on cooling from RT down to 250 K and subsequent heating up to 673 K. Inset: detail of the exothermic peaks.

3. Results and discussion

The effect of atomic order on the transformation temperatures has been firstly studied by DSC calorimetry. Figure 1 shows the DSC thermograms obtained (on cooling from RT down to 250 K and subsequent heating up to 673 K) on both PC and SC samples quenched from 1173 K. The exothermic and endothermic peaks observed below 300 K correspond to the forward (cooling) and reverse (heating) MT, respectively, whereas the anomalies around 375 K are associated with the

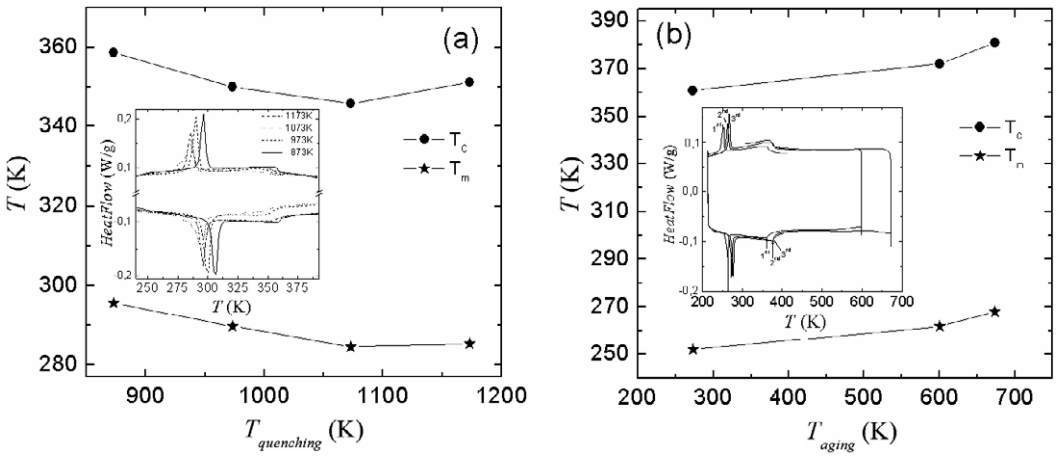

Figure 2. (a) MT and Curie temperature of the PC alloy as a function of the quenching temperature. (b) MT and Curie temperature of the SC alloy as a function of the post-quench heating temperature. The insets show the DSC thermograms performed on the samples subjected to the corresponding thermal treatments.

magnetic transition (ferro–para) taking place in the alloys. The broad exothermic peak occurring at high temperatures (figure 1, inset) corresponds to an ordering process in which the low $L2_1$ atomic order retained by quenching increases up to the equilibrium value [17].

The atomic order in the alloys may be then modified either by varying the quenching temperature or by heating quenched alloys up to temperatures above the exothermic peak. The first procedure (variation of the quenching temperature) has been applied to the PC alloy, which was subjected to 30 min annealing treatments at 873, 973, 1073 and 1173 K followed by quenching, and the second one (post-quench heating) to the SC alloy. In the latter case, three consecutive DSC thermal cycles through the MT heating up to 600 K (temperature of the exothermic peak maximum), 673 K (just above the ordering process) and 400 K have been carried out in a sample just quenched from 1173 K in order to observe '*in situ*' the evolution of both the structural and magnetic transformation temperatures. Figure 2 shows the effect of such thermal treatments on the MT and Curie temperatures of the PC (figure 2(a)) and SC (figure 2(b)) alloys, where T_m and T_C were extracted from the thermograms, as shown in figure 1. As a consequence of the increase of the degree of $L2_1$ atomic order, the transformation temperatures increase with both the decrease of the quenching temperature and the increase of the aging temperature. The fact that the transformation temperatures in the PC sample quenched from 1173 K are slightly higher than in the sample quenched from 1073 K which was related to the higher atomic order quenched in the former case as a result of a higher thermal-vacancy assistance to the ordering process [17]. It is worth noting that the variation of T_m and T_C is a little bit higher in the SC sample ($\Delta T_m^{SC} \approx \Delta T_C^{SC} \approx 16$ K versus $\Delta T_m^{PC} \approx \Delta T_C^{PC} \approx 12$ K) suggesting a larger variation of the atomic order in this alloy.

Neutron diffraction measurements have been conducted in order to quantify the effect of the thermal treatments on the atomic order in the alloys. Powder diffraction measurements of the PC alloy were carried out at 413 K (above T_C, to avoid the magnetic contribution to the reflections) on samples quenched from 873, 1073 and 1173 K as well as on a sample slowly cooled from 1173 K, using the D1B diffractometer. The diffractograms obtained in all samples correspond to the Heusler $L2_1$ structure (space group $Fm\bar{3}m$) which is inherent to the Ni–Mn–Ga austenite [7, 11]. In such diffractograms, the long-range atomic order can be easily estimated from the analysis of the integrated intensity of the superstructure reflections exclusively produced by the $L2_1$ type of ordering (those ones with odd h, k, l indices) [25]. The integrated intensity of the (111) reflection of the PC sample is shown in figure 3(a) as a function of the quenching temperature, showing that the $L2_1$ atomic order decreases with the increasing quenching temperature. It is also worth noting that the evolution of the atomic order is very similar to that of T_m and T_C (figure 2(a)). In the case of an SC alloy, neutron diffraction measurements have been performed at the D15 single-crystal diffractometer (four-circle configuration) on a sample quenched from 1173 K. Figure 3(b) shows the integrated intensity of the (111) reflections measured at 415 K on the as-quenched sample, before and after heating it up to 600 and 673 K at 10 K min^{-1} (that is, under the same thermal treatment applied in the calorimetric study). The increase of the superstructure reflection intensity with the increasing aging temperature confirms that an ordering process occurs when the sample is heated up to the DSC exothermic peak temperature. Furthermore, the behavior of both the atomic order and the transformation temperatures is also parallel under such post-quench aging treatment (figure 2(b)), as it occurs in the case of the PC alloy subjected to quenching treatments.

In order to quantify the correlation between atomic order and transformation temperatures, the degree of $L2_1$ atomic order in the alloys, η_{L2_1}, has been estimated by normalizing the intensity values in figure 3, taking into account that the slowly cooled PC sample must show the highest degree of long-range order allowed by stoichiometry (figure 3(a)) and considering that the $L2_1$ atomic disorder retained after quenching the SC alloy is completely restored once the alloy is heated up to temperatures above the DSC exothermic peak [17]. The correspondence between the transformation temperatures and

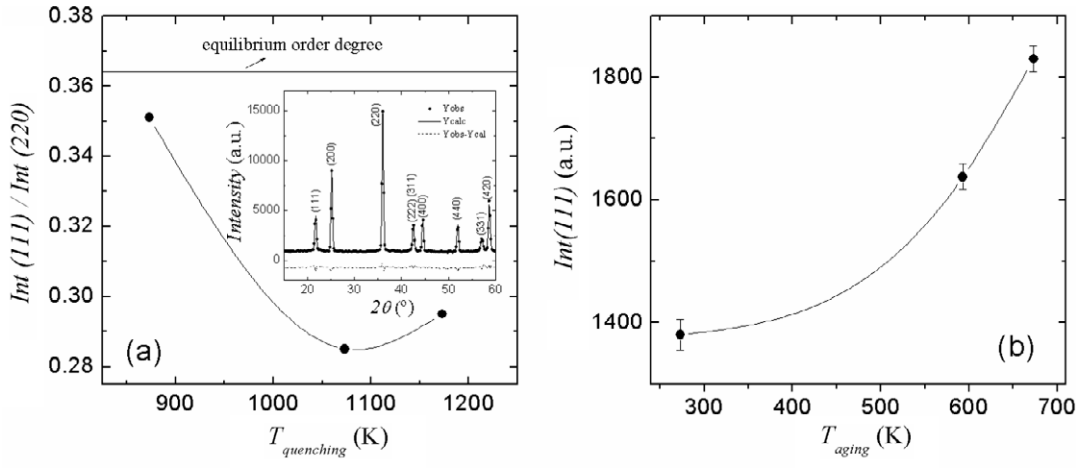

Figure 3. (a) Integrated intensity of the (111) reflections of the PC alloy (measured at 413 K) as a function of the quenching temperature. Inset: detail of the neutron diffractogram corresponding to the $L2_1$ austenite structure. (b) Integrated intensity of the (111) reflections of the SC alloy (measured at 415 K) as a function of the post-quench heating temperature.

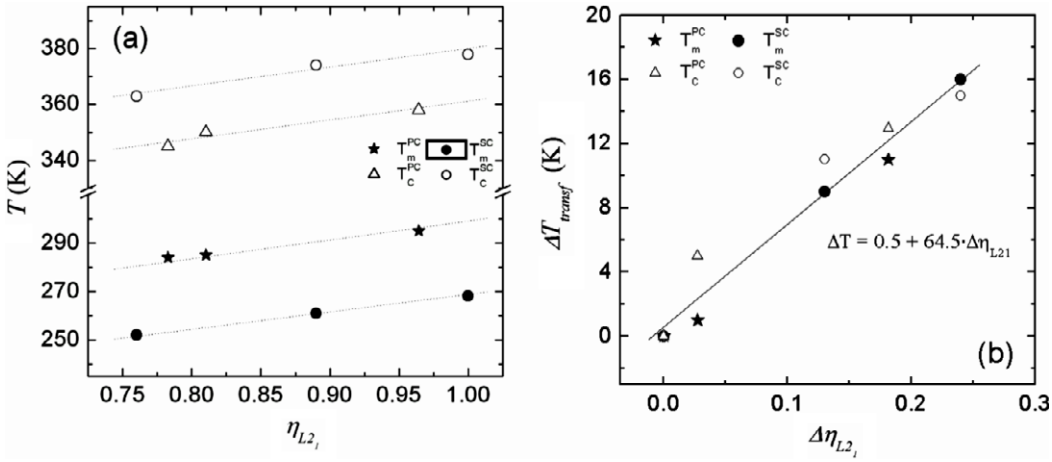

Figure 4. (a) Transformation temperatures of both alloys as a function of the degree of $L2_1$ atomic order. (b) Shift of the transformation temperatures as a function of the shift on the degree of $L2_1$ atomic order.

the degree of $L2_1$ atomic order is shown in figure 4(a.) Interestingly, the dependences of T_m and T_C on η_{L21} are almost identical for both alloys despite different thermal treatments being applied to change the atomic order. Moreover, these dependences can be approximated by straight lines which are almost parallel to each other, so the shift of T_m and T_C shows a common linear dependence on the order parameter. Therefore, a correlation between T_m, T_C and the next-nearest-neighbor order can be expressed by giving the equation describing the linear trend shown in figure 4(b).

In Ni–Mn–Ga alloys, the increase of T_C with the increasing $L2_1$ atomic order has been ascribed to the increase of the Mn–Mn coupling (responsible for the ferromagnetic character of these alloys) that takes place as a consequence of the redistribution of Mn atoms inside the $L2_1$ crystallographic cell [21, 22]. In particular, the increase of the $L2_1$ atomic order implies a decrease of the Mn atoms in the Ga sublattice that couples antiferromagnetically to the Mn at the Mn sites [23], in such a way that the total magnetic moment of the alloy increases. In this respect, figure 5 shows that, as a consequence of the thermal treatments, the saturation magnetization of both alloys, M_S, measured at 10 K essentially increases with the increasing of the $L2_1$ order parameter.

The most striking point is the fact that the change of T_m and T_C shows exactly the same dependence on η_{L2_1}. In this sense, recent measurements performed on Ni–Mn–Ga alloys with $T_m > T_C$ (that is, exhibiting an MT between two paramagnetic phases) show that, seemingly in all cases, T_m is almost unaffected by the different thermal treatments [27]. This fact seems to indicate that the structural transformation temperature reflecting the relative stability between austenite and martensite is highly influenced by the magnetism of the alloy, as suggested from theoretical studies [26]. This last observation is under the scope of more detailed studies which are in progress.

From the above results, the effect of the $L2_1$ atomic order on the relative stability between the austenitic and the martensitic phases can be quantitatively determined from the

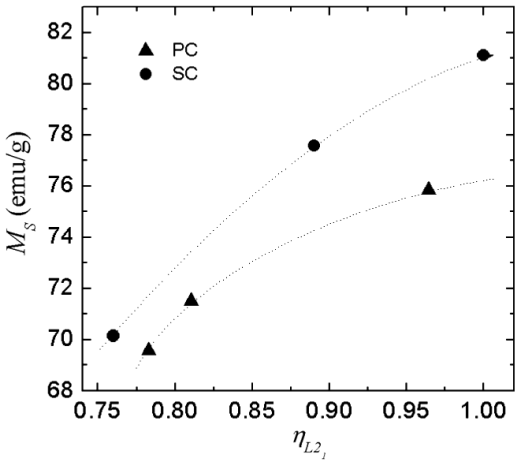

Figure 5. Saturation magnetization of both alloys at 10 K as a function of the degree of $L2_1$ atomic order.

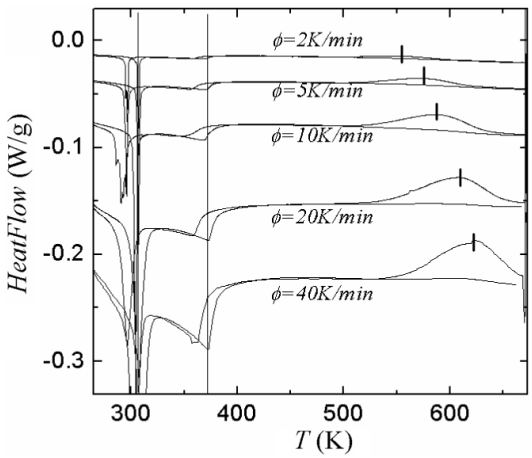

Figure 6. Thermograms obtained at different heating rates on the PC alloy quenched from 1173 K.

change in the free energy difference between both phases, $\Delta G^{\text{aust}\to\text{mart}}$ [28]. This change can be represented as

$$\delta\Delta G^{\text{aust}\to\text{mart}} = \Delta S^{\text{aust}\to\text{mar}}\delta T_{\text{m}} \tag{1}$$

where $\Delta S^{\text{aust}\to\text{mart}}$ is the entropy change per unit volume associated with the MT and δT_{m} is the shift of the MT temperature due to the variation of the atomic order. The latter shift can be expressed as $\delta T_{\text{m}} = \alpha\delta\eta_{\text{L2}_1}$, where α is the slope of the linear curve shown in figure 4(b), so equation (1) yields

$$\delta\Delta G^{\text{aust}\to\text{mart}} = \Delta S^{\text{aust}\to\text{mar}}\alpha\delta\eta_{\text{L2}_1}. \tag{2}$$

The rate of the free energy change as a function of the degree of $L2_1$ atomic order can be then expressed as

$$\frac{\delta\Delta G^{\text{aust}\to\text{mart}}}{\delta\eta_{\text{L2}_1}} = \Delta S^{\text{aust}\to\text{mar}}\alpha. \tag{3}$$

The entropy change at the MT has been calculated from the DSC thermograms obtained on both alloys subjected to the corresponding thermal treatments as $\Delta S^{\text{aust}\to\text{mart}} = \Delta H^{\text{aust}\to\text{mart}}/T_0$, where $\Delta H^{\text{aust}\to\text{mart}}$ is the enthalpy change at the MT and T_0 represents the mean value between reverse and forward MTs. A mean value $\Delta S^{\text{aust}\to\text{mart}} = -0.012 \pm 0.1$ J g^{-1} K^{-1} has been obtained in both alloys, so equation (3) yields

$$\frac{\delta\Delta G^{\text{aust}\to\text{mart}}}{\delta\eta_{\text{L2}_1}} = -0.774\ \text{J g}^{-1} \approx -46.44\ \text{J mol}^{-1}. \tag{4}$$

This quantitative evaluation of the effect of atomic order on the MT in Ni–Mn–Ga alloys, the first of this kind, can be compared, for example, with the result on the relative stability between the 14M and 2M martensites in Ni–Mn–Ga alloys, $\delta\Delta G^{14\text{M}\to 2\text{M}}/\delta\eta_{\text{L2}_1} \approx -25$ J mol^{-1}, obtained by Seguí *et al* [28]. It can be seen that the rate of the free energy change as a function of the degree of $L2_1$ atomic order is considerably higher (in absolute values) in the case of the MT. Incidentally, it is worth noting that, under similar variations of η_{L2_1}, the shift of the 14M → 2M intermartensitic transformation temperature is much higher than the shift of the MT temperature ($\Delta T^{14\text{M}\to 2\text{M}} \approx 60$ K versus $\Delta T^{\text{aust}\to\text{mart}} \approx 16$ K). This is because the different martensitic structures are energetically closer than austenite and martensite, as inferred from the fact that the entropy change at the intermartensitic transformation is almost 10 times lower than the MT entropy [29].

The kinetics of the $L2_1$ ordering process associated with the high temperature DSC exothermic peak has also been investigated. In particular, the activation energy of such a process has been determined using the well-known Kissinger's method, which is based on the analysis of the variation of the DSC peak temperature as a function of the heating rate. In this method the activation energy of a thermally activated process can be obtained from the equation

$$\text{Ln}\left(\frac{\phi}{T_{\text{P}}^2}\right) = -\frac{E_{\text{a}}}{RT_{\text{P}}} + B \tag{5}$$

where T_{P} is the temperature of the peak maximum, ϕ is the heating rate, R is the ideal gas universal constant ($R = 8.314$ J K^{-1} mol^{-1}), E_{a} is the activation energy and B is a constant. The DSC thermograms obtained on a PC sample quenched from 1173 K for different heating rates are shown in figure 6. The thermograms consist of two consecutive heating curves recorded between 265 and 673 K.

It can be observed that the temperature of the exothermic peak increases with the increasing heating rate, whereas neither the MT nor the magnetic transition temperatures change with the heating rate (as expected due to the athermal character of both transformations). Furthermore, the absence of an exothermic peak on the second heating curve confirms the irreversible character of the ordering process. Figure 7 shows the plot of $\text{Ln}(\phi/T_{\text{P}}^2)$ against $1/T_{\text{P}}$ for two PC samples quenched from 1173 K and 873 K (figures 7(a) and (b), respectively). Taking into account that the slopes of the linear curves shown in the graphs are equal to E_{a}/R (equation (5)), the activation energies of the respective post-quench ordering processes are $E_{\text{a}} = 114 \pm 3$ K J mol^{-1} (=1.18 eV) for the

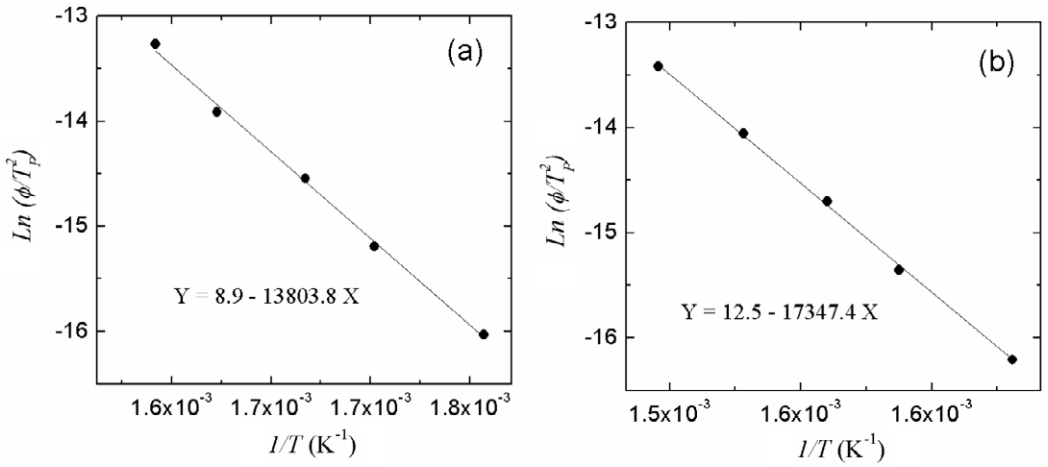

Figure 7. Evolution of $\mathrm{Ln}(\phi/T_\mathrm{P}^2)$ against $1/T_\mathrm{P}$ for the PC alloy quenched from (a) 1173 and (b) 873 K.

sample quenched from 1173 K, and $E_\mathrm{a} = 144 \pm 3$ K J mol^{-1} for the sample quenched from 873 K.

It is interesting to note that these values are very close to the experimental value of the activation energy of the Mn self-diffusion ($E_\mathrm{a}^\mathrm{Mn} = 141 \pm 5$ K J mol^{-1}) obtained recently from radioactive tracer measurements performed on a stoichiometric Ni_2MnGa alloy [30]. This similarity is reasonable, bearing in mind that the ordering process consists mainly in the diffusion of Mn atoms from the Ga sublattice to their own sublattice [17, 19]. The fact that the activation energy of the ordering process taking place in the alloy quenched from 873 K is higher than that on the alloy quenched from 1173 K could be related to the presence of a higher concentration of non-equilibrium vacancies in the latter case, which may favor the ordering process. In fact, the activation energy of the Mn self-diffusion is almost the same as the energy of the ordering process in the alloy quenched from 873 K, in which the vacancies concentration may be assumed to be much closer to the equilibrium value.

4. Summary and conclusions

The effect of atomic order on both the martensitic and magnetic transformations of near-stoichiometric Ni_2MnGa alloys has been studied. Calorimetric, magnetic and neutron diffraction measurements have been performed on polycrystalline and single-crystalline alloys subjected to different thermal treatments. It is found that, irrespective of the thermal treatments, both transformation temperatures show exactly the same linear dependence on the degree of $L2_1$ atomic order. A quantitative correlation between martensitic transformation and atomic order has been established, and from it the effect of the $L2_1$ atomic order degree on the relative stability between the austenite and martensitic phases has been calculated in terms of the free energy change. On the other hand, the activation energy of the post-quench ordering process taking place in these alloys has also been calculated. The obtained value agrees with the activation energy of the Mn self-diffusion process.

Acknowledgments

This work was carried out with the financial support of the Spanish 'Ministerio de Ciencia y Tecnología' and FEDER (project nos. MAT2006-12838, MAT2007-61621, MAT2008-06542 and MAT2009-07928) and the Government of Navarra (project entitled 'Efecto magnetocalórico en aleaciones con memoria de forma ferromagnéticas'). The Institute Laue-Langevin D1B installation and the Spanish CRG D15 installation are acknowledged for the allocated neutron beamtime (Exp. 5-24-262 and CRG-D15-08-118). The financial support from the Department of Education, Basque Government (project no. IT-347-07), is gratefully acknowledged.

References

[1] O'Handley R C, Murray S J, Marioni M, Nembach H and Allen S M 2000 *J. Appl. Phys.* **87** 4712
[2] Ullakko K, Huang J H, Kantner C, O'Handley R C and Kokorin V V 1996 *Appl. Phys. Lett.* **69** 1966
[3] Planes A, Mañosa Ll and Acet M 2009 *J. Phys.: Condens. Matter* **21** 233201
[4] Liu Z H, Liu H, Zhang X X, Zhang X K, Xiao J Q, Zhu Z Y, Day X F, Liu G D, Chen J L and Gu G H 2005 *Appl. Phys. Lett.* **86** 182507
[5] Sozinov A, Likhachev A A, Lanska N and Ullakko K 2002 *Appl. Phys. Lett.* **80** 1746
[6] Brown P J, Bargawi A Y, Crangle J, Neuman K U and Ziebeck K R A 1999 *J. Phys.: Condens. Matter* **11** 4715
[7] Brown P J, Crangle J, Kanomata T, Matsumoto M, Neumann K U, Ouladdiaf B and Ziebeck K R A 2002 *J. Phys.: Condens. Matter* **14** 10159
[8] Pons J, Chernenko V A, Santamarta R and Cesari E 2000 *Acta Mater.* **48** 3027
[9] Jin X, Marioni M, Bono D, Allen S M, O'Handley R C and Hsu T Y 2002 *J. Appl. Phys.* **91** 8222
[10] Chernenko V A 1999 *Scr. Mater.* **40** 523
[11] Webster P J, Ziebeck K R A, Town S L and Peak M S 1984 *Phil. Mag.* B **49** 295
[12] Islam Z, Haskel D, Lang J C, Srajer G, Lee Y, Harmon B N, Goldman A I, Schlagel S L and Lograsso T A 2006 *J. Magn. Magn. Mater.* **303** 20

[13] Overholser R W, Wuttig M and Neumann D A 1999 *Scr. Mater.* **40** 1095
[14] Khovailo V V, Takagi T, Vasil'ev A N, Miki H, Matsumoto M and Kainuma R 2001 *Phys. Status Solidi* **183** R1
[15] Söderberg O, Friman M, Sozinov A, Lanska N, Ge Y, Hämäläinen M and Lindroos V K 2004 *Z. Met.kd.* **95** 724
[16] Schlagel D L, Wu Y L, Zhang W and Lograsso T A 2000 *J. Alloys Compounds* **312** 84
[17] Sánchez-Alarcos V, Pérez-Landazábal J I, Recarte V and Cuello G J 2007 *Acta Mater.* **55** 3883
[18] Tsuchiya K, Ohtoyo D, Umemoto M and Ohtsuka H 2000 *Trans. Mater. Res. Soc. Japan* **25** 521
[19] Kreissl M, Neumann K U, Stephens T and Ziebeck K R A 2003 *J. Phys.: Condens. Matter* **15** 3831
[20] Goryczka T, Gigla M and Morawiec H 2006 *Int. J. Appl. Electromagn. Mech.* **23** 81
[21] Richard M L, Feuchtwanger J, Allen S M, O'Handley R C, Lázpita P, Barandiarán J M, Gutiérrez J, Ouladdiaf B, Mondelli C, Lograsso T and Schlagel D 2007 *Phil. Mag.* **87** 3437
[22] Sánchez-Alarcos V, Pérez-Landazábal J I, Gómez-Polo C and Recarte V 2008 *J. Magn. Magn. Mater.* **320** e160
[23] Enkovaara J, Heczko O, Ayuela A and Nieminen R M 2003 *Phys. Rev.* B **67** 212405
[24] UNPN-E007 Feder Project 2003
[25] Planes A, Mañosa Ll, Vives E, Rodriguez-Carvajal J, Morin M, Guénin G and Macqueron J L 1992 *J. Phys.: Condens. Matter* **4** 553
[26] Buchelnikov v D, Taskaev S V, Zagrebin M A, Zayak A T and Takagi T 2007 *J. Magn. Magn. Mater.* **316** e591
[27] Sánchez-Alarcos V 2008 *PhD Thesis* Universidad del País Vasco, EHU (Spain)
[28] Seguí C, Pons J and Cesari E 2007 *Acta Mater.* **55** 1649
[29] Chernenko V A, Seguí C, Cesari E, Pons J and Kokorin V V 1998 *Phys. Rev.* B **57** 2659
[30] Erdélyi G, Mehrer H, Imre A W, Lograsso T A and Schlagel D L 2007 *Intermetallics* **15** 1078